Angle-Resolved Scatter Measurements of Laser Damaged DKDP Crystals using a Bi-Directional Scatter Diagnostics

R. Fluck, P.Wegner, L. Sheehan, and L.A. Hackel

U.S. Department of Energy

Lawrence
Livermore
National
Laboratory

December 22, 2000

This report has been reproduced directly from the best available copy.

Available electronically at http://www.doc.gov/bridge

Available for a processing fee to U.S. Department of Energy
And its contractors in paper from
U.S. Department of Energy
Office of Scientific and Technical Information
P.O. Box 62
Oak Ridge, TN 37831-0062
Telephone: (865) 576-8401
Facsimile: (865) 576-5728
E-mail: reports@adonis.osti.gov

Available for the sale to the public from
U.S. Department of Commerce
National Technical Information Service
5285 Port Royal Road
Springfield, VA 22161
Telephone: (800) 553-6847
Facsimile: (703) 605-6900
E-mail: orders@ntis.fedworld.gov
Online ordering: http://www.ntis.gov/ordering.htm

OR

Lawrence Livermore National Laboratory
Technical Information Department's Digital Library
http://www.llnl.gov/tid/Library.html

Angle-resolved scatter measurements of laser damaged DKDP crystals using a bi-directional scatter diagnostics

R. Fluck, P. Wegner, L. Sheehan, L. A. Hackel
Lawrence Livermore National Laboratory
POBox 808, L-438, Livermore, CA 94550, USA
Tel: (925) 422 0309, Fax: (925) 423 9242

ABSTRACT

We built a bi-directional scatter diagnostics to measure and quantify losses due to scattering and absorption of harmonic conversion crystals (DKDP) for the National Ignition Facility (NIF). The main issues to be addressed are (1) amount of total energy reaching the target if the target hole was +/-200 μrad in size, (2) distribution of energy inside the target hole, (3) collateral damage of other optics by scattered light. The scatter diagnostics enables angle-resolved measurements at 351 nm, and is capable of both near specular transmission and large angle scatter measurements. In the near specular setup, the transmission can be measured within +/-65 μrad up to +/-60 mrad acceptance angle. A silicon photo detector and a scientific-grade CCD camera provide total energy and energy distribution. A linear swing arm detection system enables large angle scatter measurements of 360°, in principal, with step sizes as small as 0.01° and different collection angle ranging between 1 and 20 mrad. In this paper, scatter effects from laser damage and final finishing process of DKDP are discussed.

1. INTRODUCTION

The National Ignition Facility (NIF) has strong interest in measuring losses due to scattering in key areas of the laser system. Specifically in the final optics assembly, which includes harmonic conversion crystals and several fused silica optics. We built a bi-directional scatter diagnostics to address the following issues:

The entrance hole of the target has a diameter of ~3 mm. This results in an acceptance angle of +/-200 μrad for optics in the final optics assembly. Commercial available photometers usually are limited to an acceptance angle of a few mrad. Our scatterometer was especially designed to measure transmission within an acceptance angle as small as +/-65 μrad adjustable up to 58 mrad.

The distribution of the energy within the +/-200 μrad can affect loading on the target entrance hole. A 16 bit, scientific-grade camera combined with an integrated Schlieren-technique provides beam or scatter images, and thus energy distribution, over a wide range.

Stray radiation can have adverse effects on the system performance. The illuminated walls of the mechanical assemblies can cause material ablation and optics contamination. Furthermore, an enhanced beam near field contrast increases the risk of damaging collateral optics. The scatterometer features a linear swing arm design, which enables angular resolved scatter measurements for 360°, in principal.

In this paper, we discuss the instrument design, which meets the requirements needed to investigate NIF optics. In chapter 3, laser damaged DKDP crystals and DKDP crystals with different surface quality are investigated. The angle resolved scatter and transmission measurements give insight about the scatter level of current NIF optics.

2. INSTRUMENT DESCRIPTION: THE BI-DIRECTIONAL SCATTER DIAGNOSTICS

Figure 1 shows a schematic layout of the scatterometer. An Argon ion laser with a nearly diffraction limited gaussian beam at 351 nm is used as the light source. A spatial filter defines the angular extent of the laser source by eliminating highly divergent light and scatter from the source and optics in front of the filter. A two mirror telephoto system expands and focuses the beam at a low divergence through the sample onto the far field plane. The scatter measurements are performed in the far field. The aperture at the far field plane defines the acceptance angle and can be chosen to be +/-200 μrad, for example. The scatterometer features at that point two options: a near specular diagnostics (NSD) which enables energy transmission and distribution measurements, and a large angle diagnostics (LAD) which sits on a linear swing arm and enables angular resolved scatter measurements.

Angel resolved measurements within an acceptance angle as small as +/-200 μrad require a high-quality beam with low divergence. In our setup, the gaussian beam spans +/-17 μrad at the far field plane, as defined by focusing optics geometry, beam size on sample, and distance from sample to focus. The further away the sample is placed from the far field the better

the angular resolution. However, the beam size on the sample should be not too large, but chosen in such a way, that smaller features or defined areas as laser damage spots can still be separately investigated. The sample is placed 600 mm from the far field plane where the beam diameter is about 13 mm. These design parameters allow near specular measurements with high angular resolution for very small acceptance angle. The spatial filter limits the effective angular extent of the source to +/-65 µrad, while maintaining a gaussian beam profile with low scatter in the near field. The telephoto optical design enables the expansion to a large beam with low divergence within a short distance. Additionally, the telephoto is designed to image the spatial filter to the far field plane. Super polished mirrors in an astigmatism compensating geometry were used, which feature low scatter, low aberration, and no lens ghosts.
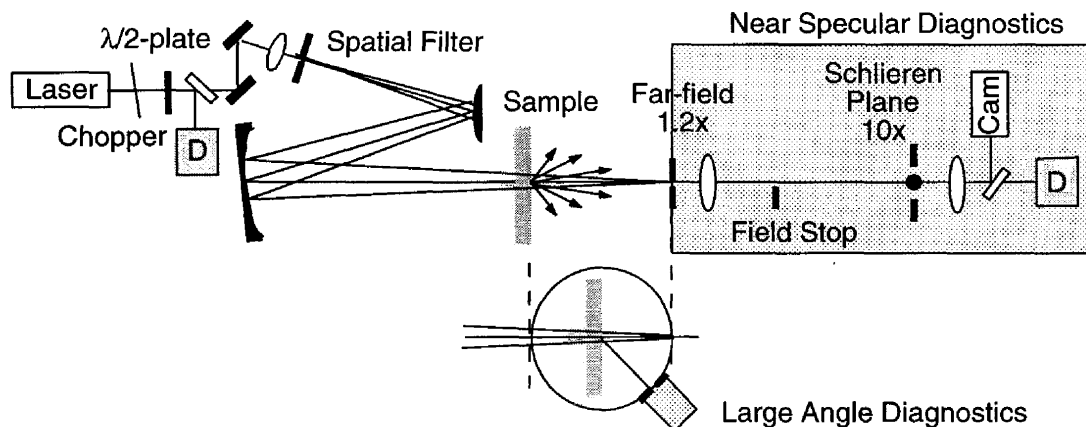

Fig. 1: Schematic layout of the scatterometer with near specular and large angle diagnostics option.

The near specular diagnostics is designed to image the far field onto the Schlieren plane using a 10 times magnifying telescope. The incorporation of a Schlieren technique allows the use of reasonable sized balls to block the intense specular beam and to increase the dynamic range for the near specular scatter distribution. The Schlieren plane is imaged onto a scientific grade CCD camera featuring back illumination, 1024x1024 pixels, and 16 bit. An integrating sphere with a Si-detector is used to measure the field transmission. A high signal to noise ratio is provided by using lock-in techniques. A chopper and reference detector in front of the spatial filter provide absolute measurements.
A field stop at the image plane of the sample insures that only scattered light from a selected sample area is detected.
Figure 2 shows the beam profile of the gaussian beam which represents the instrument signature. The data was taken by using the Schlieren technique. The CCD camera itself has a dynamic range of 4.5 orders of magnitudes. Using the Schlieren technique the dynamic range was enhanced by 3 to 4 orders of magnitude. At about +/-65 µrad the cut off of the spatial filter can be observed. At the far field aperture edge, which was in this case at +/-162 µrad, the signal drops into the noise level.
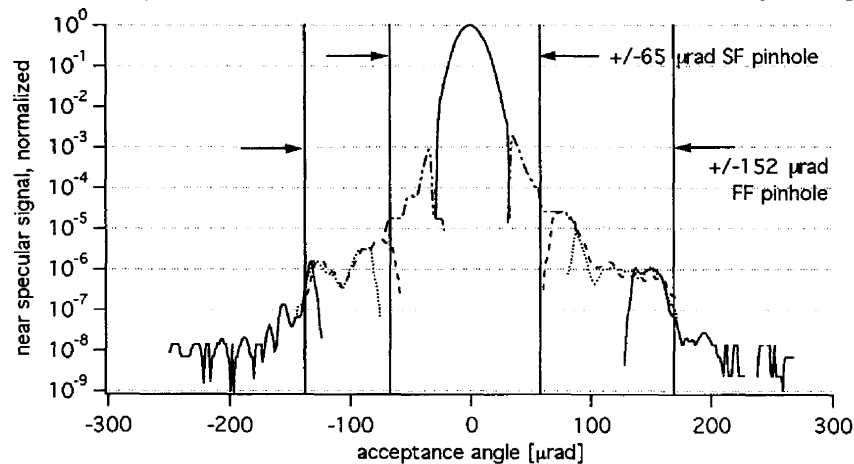

Fig. 2: Near specular beam profile using Schieren technique to enhance the dynamic range.

The signal within the far field aperture but outside the spatial filter is about 5 orders of magnitude lower than the specular beam. Some potential scatter light from the last turning mirror just in front of the spatial filter might be caught on the large size telephoto mirrors, and some low scatter from the telephoto mirrors itself might cause this back ground noise of the system.

The top row of Figure 3 shows the CCD pictures of the beam, each taken with the same far-field aperture, but with different size of Schlieren balls and different calibrated filters in front of the camera. The second row shows the corresponding images of the far field aperture and Schlieren balls when using a scattered light source for illumination instead of the laser beam. This Figure shows that the largest far field aperture cannot exceed an acceptance angle of +/-355 rad in this optical configuration.
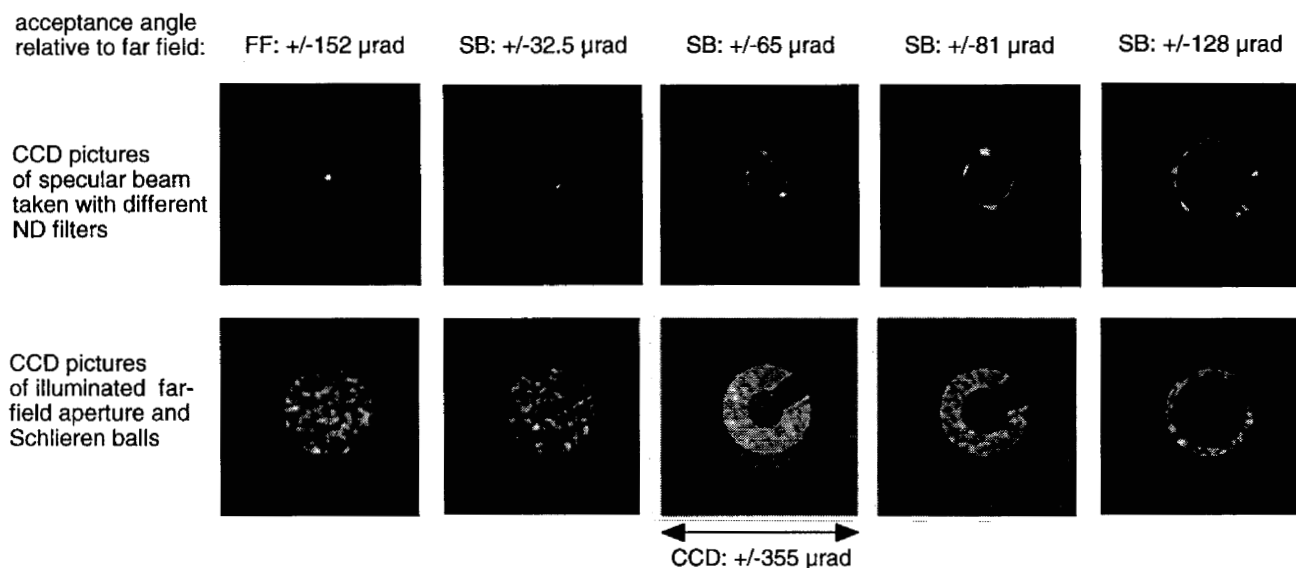

Fig. 3: CCD pictures of near specular beam (upper row) and images of aperture and Schlieren balls using a scattered light source for illumination (lower row). The acceptance angle is given for the far-field aperture (FF), the Schlieren balls (SB) and the CCD size (CCD), in each case relative to the far-field plane.

The large angle diagnostics has the same optical design principal as the near specular diagnostics, however without the Schlieren option and on a much smaller scale. The far field is imaged onto a Si-detector and a field stop can be inserted to select the sample area. The LAD sits on a linear swing arm centered underneath the sample. It is driven by a Newport motion controller, which can perform angular steps as small as 0.01° and has an angular step size accuracy of 0.02°. In the LAD setup the sample holder is placed only 300 mm from the far field. That enables an angular scatter measurement for 360°, thus, forward and backward scattering can be investigated. Forward scattering can be collected within -70° to 65° with the specular beam centered at 0°. Negative angles from –110° to –245° show the backward scattering with the specular beam at -180°. Scattering from angles outside this range cannot be collected due to mechanical constrictions. Currently, we have 3 different aperture sizes available with a diameter corresponding to a collection angle of 20/6.7/0.7 mrad. The apertures are drilled into a cone with a half-angle of 40°. This hardware design should prevent recollection of scattered light originating when the specular beam hits LAD hardware. Nevertheless, data collected between +/-2.5° should not be used for data analysis.

Figure 4 shows the scatter signal as a function of scatter angle. These scans were performed without a sample. They represent the instrument signature of the scatterometer for the different apertures. The noise level is 8 orders of magnitudes lower than the specular peak. A decreased collection angle (decreased aperture size) not only increases the angular resolution but also reduces the instrument signature. The two bumps in the backward scatter signal are scatter from the specular beam from the enclosure wall. No ideal material was found so far to fully prevent this scatter light. The drop at 180° is due to the LAD hardware blocking the specular beam.
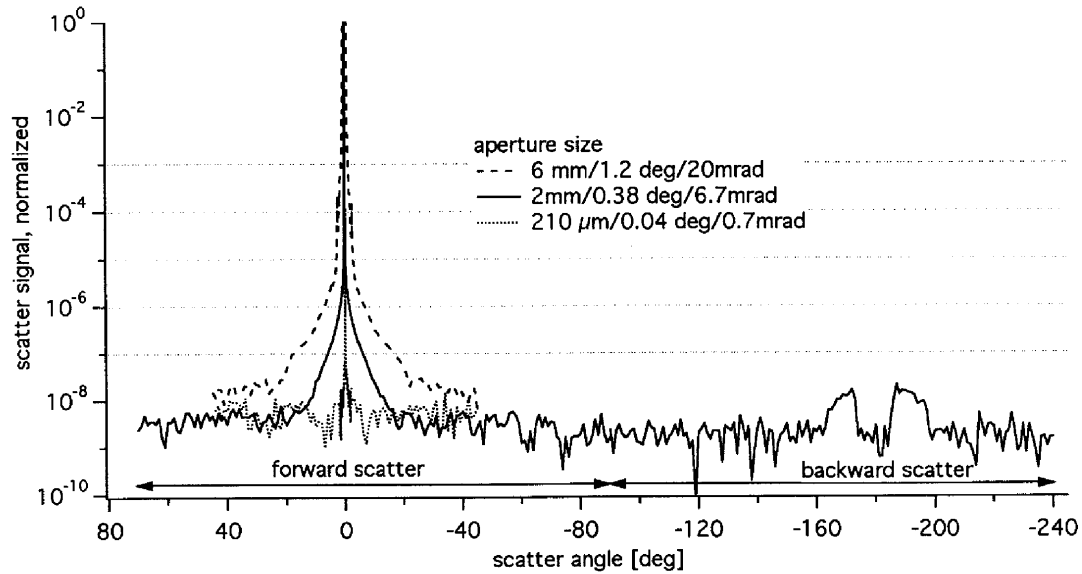
Fig. 4: Instrument signature of LAD taken with different apertures. The angular step size was 0.1° and 0.01° in the near specular regime and 1° elsewhere.

3. INVESTIGATION OF DKDP SAMPLES

There was a lot of progress in the development of large size DKDP crystals [ref], nevertheless there are some defects left from crystal growth and final finishing process. NIF relies on the electro-optical and nonlinear properties of KDP and DKDP optics as well as high optical transmittance. Since NIF is composed of 192 laser beams each of which has three crystals, it is very important to minimize transmittance losses from surfaces and bulk. There are many different potential sources for defects in DKDP, which will cause scatter - as for example bulk inclusion and cracks from the growth process, surface roughness and defects caused by the final finishing process, or bulk defects initiated by laser exposure. In this paper, we present large angle and near specular scatter measurements of samples from a high temperature, rapid grown DKDP boule. The samples are 5cmx5cm, tripler cut and uncoated. In the next section, a bare and a fogged DKDP sample are discussed, and in the following section scatter from laser exposed DKDP is discussed.

The first set of experiments was performed on two samples, which feature diamond turning lines from the final finishing process. One of the sample is a bare sample (BD7-41), the other one is fogged (BD7-60). Some potential reasons/origin for fogging. For both samples near specular transmission was measured using 3 different far field apertures. Figure 5 shows the transmission as a function of full acceptance angle on a log scale. The solid line represents the calculated Fresnel loss for both ordinary-polarized (o) and extraordinary-polarized (e) electric field vectors. The circles represents the bare sample, the squares the fogged one. As expected, the fogged sample shows lower transmission than the bare sample. At the NIF required acceptance angle of 400 μrad (+/-200 μrad), the bare sample shows about 0.5% loss and the fogged sample an additional 0.7%. The loss includes scatter from both surfaces and bulk as well as absorption loss if present. For a larger acceptance angle as 120 mrad the transmission increases because more scattered light can be collected. The third data point at >1000 mrad was actually taken using a different instrument which is capable to measure total integrated loss between 120 mrad and about 45°. The main conclusion from this measurement is that the instrument acceptance angle is a very important parameter and always needs to be included in the data interpretation of NIF optics.
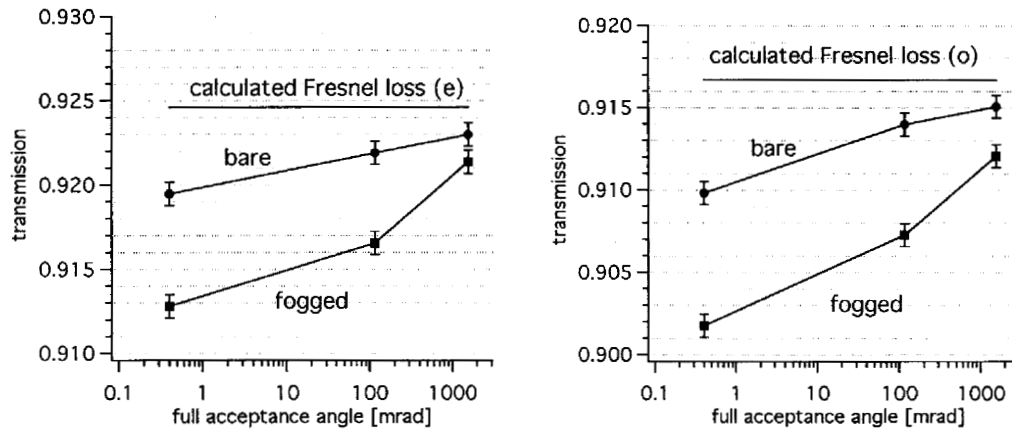
Fig. 5: NSD transmission for different acceptance angle

Large angle scans were performed on the bare sample to show the angular distribution of the scattered light. Figure 6 shows the scatter signal as a function of scatter angle. The scattered signal was collected using a 6 mm aperture. Two scatter scans of the samples are depicted - the sample was rotated 90° from one scan to the other - as well as an air scan. The solid line shows a very distinct picture of peaks. The regular spacing of the peaks indicates a periodic structure on the sample. Using the grating equation, the period of grating can be estimated to about 3.8 μm. If we assume a sinusoidal grating the first scatter peak which is about 4 orders of magnitudes smaller than the incident beam, predicts a grating amplitude of about 0.6 μm. This large-angle scan clearly resolves scattering from diamond turning grooves, a result from the final finishing process. Only about 0.01% of the energy is located in each of the first scatter peaks at a scatter angle of 5°. That scatter signal would corresponds to an energy of about 1 J in the NIF final optics assembly.

The scan (dashed line) which was performed perpendicular to the diamond turning scatter (DTS) axis shows the same large angle scatter signal however lacks the scatter peaks from the other sample scans. Its scatter signal is slightly larger than the instrument signature, which indicates that there is scatter from the DKDP sample, which has an origin other than the diamond turning lines.

The large aperture was chosen to be able to collect all scattered light of each single peak. This configuration allows us to predict the grating amplitude. However, it results in reduced angular resolution. Figure 6b shows the scans taken with 3 different aperture sizes. Higher angular resolution results in smaller peak width but also results in a lower peak value, because part of the peak energy perpendicular to the scan direction is not captured anymore.
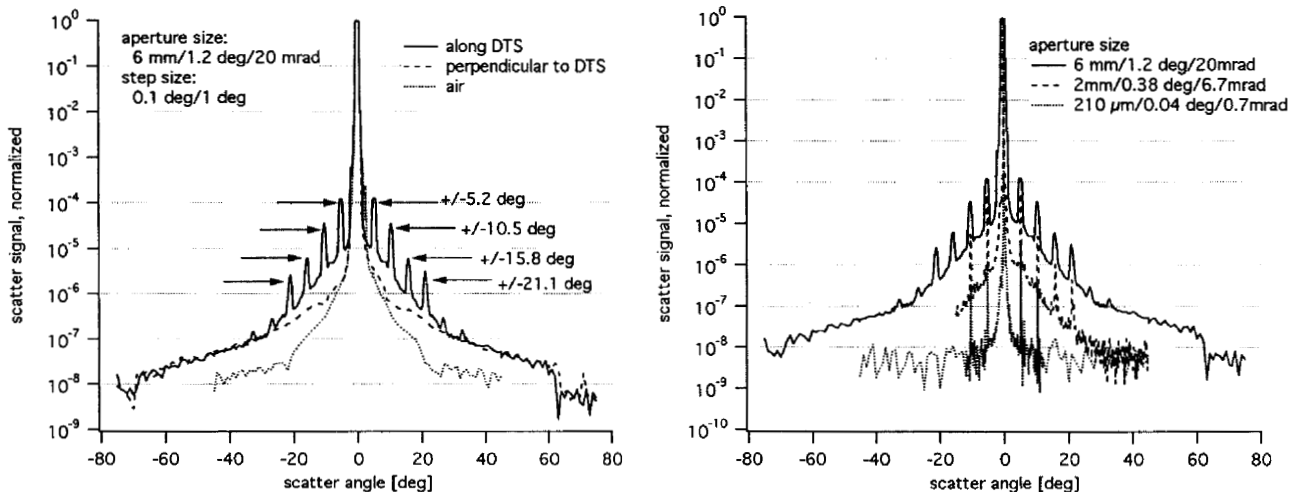

Fig. 6: Large angle scattering from the bare DKDP sample, left: different sample orientations, right: different collection apertures.

Measurements with an atomic force microscope (AFM) were performed to confirm the results above. Figure 7 shows a 30 μm by 30 μm scan of the bare sample. The picture clearly shows the diamond turning lines. The graph on the right side shows a cross section perpendicular to the lines. The distances between the peaks indicated by cursors are 3.75 μm and the amplitude varies between 0.5 μm to a few μm. These values confirm the result achieved by the scatterometer. The advantage of the scatterometer is that a larger area can be investigated. Thus, the scatterometer provides a more efficient measurement technique and will reveal more about the average scattering of NIF optics.
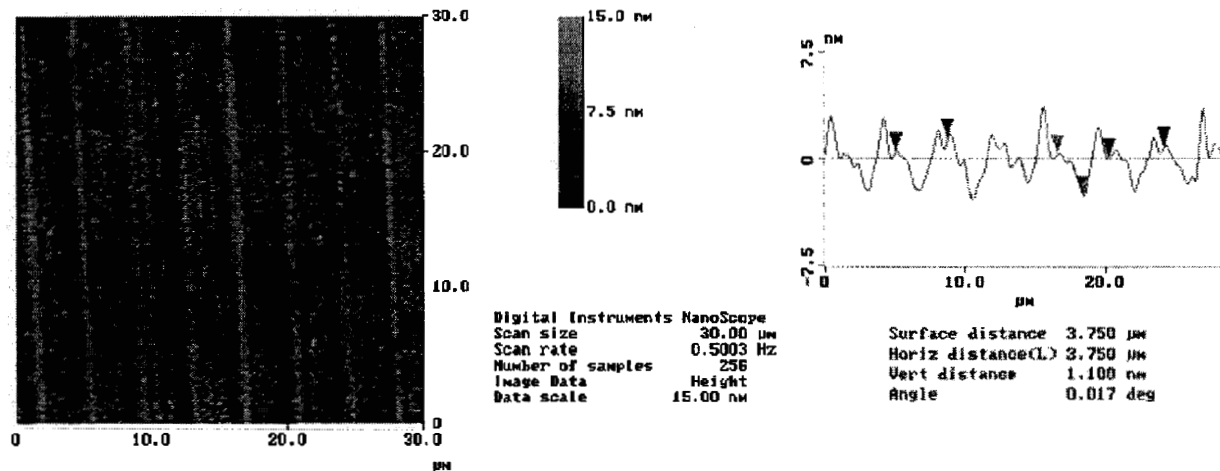

Fig. 7: AFM picture of bare DKDP sample with amplitude profile cross section.

In this section, scatter from laser exposed DKDP will be discussed as a function of laser fluence and pulse duration. The samples were exposed to single laser shots at 351 nm with average fluences from 4 to 8 J/cm2 for pulse durations of 1, 3, and 10 ns (BD7-PY-37, BD7-PY-27, and BD7-4). More information on how the experiments were conducted and how the pulse scaling analysis was performed can be found in two other papers presented in this proceeding [ref]. In this paper we only focus on scatter loss from the different damage sites. Figure 8 depicts dark field images of the laser exposed samples. The pictures show the degree of white light scatter from damage sites.
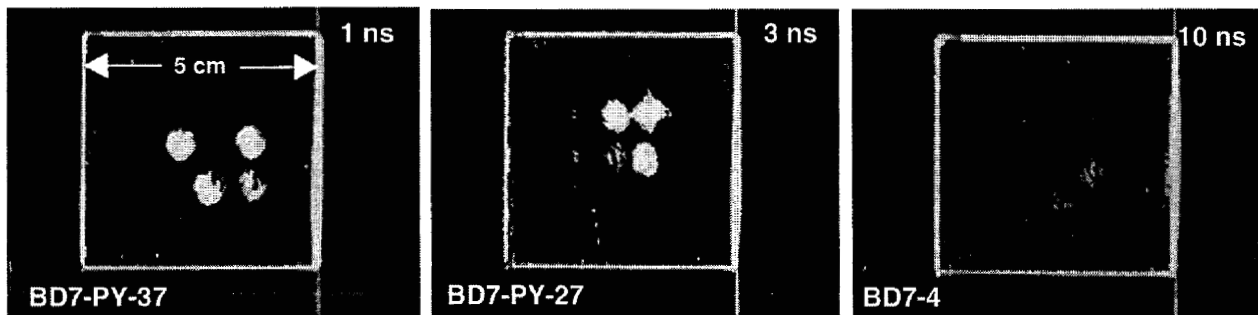

Fig. 8: Dark field images of laser exposed DKDP samples.

The transmission was measured within an acceptance angle of +/-200 μrad for all the damage spots on all 3 samples. With increased fluence significant loss can be observed, up to 50% (Fig. 9, left). The right graph of Figure 9 plots the scattered light and loss outside of +/-200 μrad on a log scale. Again, the loss for the NIF acceptance angle is on the order of 0.5% for an undamaged site (0 fluence).
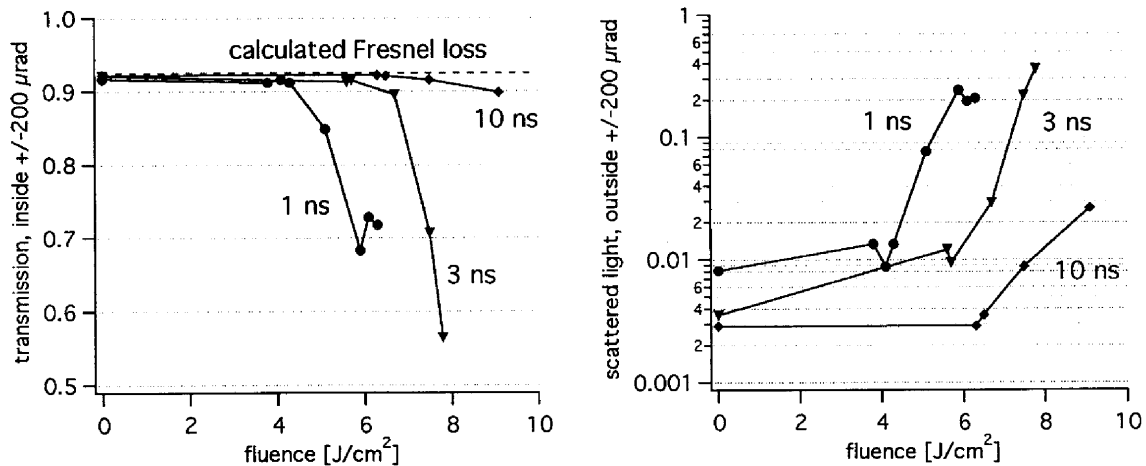
Fig. 9: Near specular transmission within and scatter loss outside of NIF specified acceptance angle of +/-200 μrad.

Large angle scatter measurements were performed of damaged and undamaged sites on the 1 ns sample (BD7-PY-37) using a 6 mm aperture. As expected from the near specular transmission measurement, the amount of scattered light increases with increasing fluence. The scatter signal drops with the same power function for all fluence levels. The cut-offs at 65° and 70° are due to blocking of the scattered light by mechanical hardware. As already noted from LAD measurements of the bare sample, undamaged areas of the sample show a residual scatter signal significantly higher than the instrument signature.
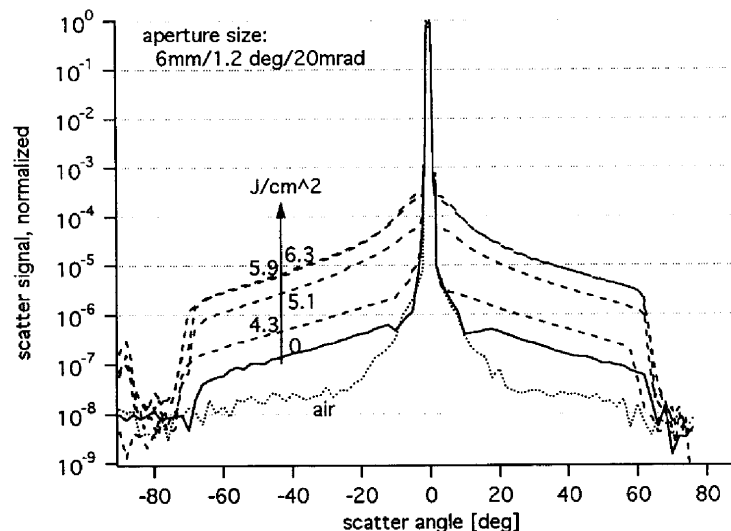

Fig. 10: Large angle scattering from different sites of laser damaged DKDP sample.

4. SUMMARY

We developed a scatterometer to measure transmission of DKDP samples within the NIF specified acceptance angle of +/-200 xrad with an accuracy better than 0.1%. Additionally, this instrument provides angle resolved scatter measurement of 360° with an angular accuracy of 0.002°. We used this instrument to correlate bulk damage of laser exposed DKDP with transmission and scatter loss. This work will lead to improved specifications for allowable bulk damage of NIF optics. Generally, the scatterometer is used at the Lawrence Livermore Laboratory as a reference for absolute transmission measurements and will serve as a scientific tool to investigate defects in DKDP and its impact on NIF performance.